

# A 10 GHz Y-Ba-Cu-O/GaAs Hybrid Oscillator Proximity Coupled to a Circular Microstrip Patch Antenna

Norman J. Rohrer, M. A. Richard, *Student Member, IEEE*, George J. Valco, *Member, IEEE*, and Kul B. Bhasin, *Senior Member, IEEE*

**Abstract**—A 10 GHz hybrid Y-Ba-Cu-O/GaAs microwave oscillator proximity coupled to a circular microstrip antenna has been designed, fabricated and characterized. The oscillator was a reflection mode type using a GaAs MESFET as the active element. The feedline, transmission lines, rf chokes, and bias lines were all fabricated from  $\text{YBa}_2\text{Cu}_3\text{O}_{7-x}$  superconducting thin films on a  $1\text{ cm} \times 1\text{ cm}$  lanthanum aluminate substrate. The output feedline of the oscillator was wire bonded to a superconducting feedline on a second  $1\text{ cm} \times 1\text{ cm}$  lanthanum aluminate substrate, which was in turn proximity coupled to a circular microstrip patch antenna. Antenna patterns from this active patch antenna and the performance of the oscillator measured at 77 K are reported. The oscillator had a maximum output power of 11.5 dBm at 77 K, which corresponded to an efficiency of 10%. In addition, the efficiency of the microstrip patch antenna together with its high temperature superconducting feedline was measured from 85 K to 30 K and was found to be 71% at 77 K, increasing to a maximum of 87.4% at 30 K.

## I. INTRODUCTION

The application of high temperature superconducting (HTS) thin films to microwave circuits is advantageous since the films have a lower surface resistance than gold or copper at microwave frequencies. Passive circuits such as ring resonators [1], [2], filters [3], transmission lines [4], and antennas [5] fabricated from HTS films have shown substantial improvements in performance over identical circuits fabricated with normal metals. Several authors have suggested that HTS technology may be very beneficial in phase-array antenna systems [6], [7]. To date, a limited amount of work in the area of passive microstrip antennas has been reported [5]. However, for HTS to be useful in phased array antennas, active circuits such as oscillators, phase shifters and power amplifiers, will need to be integrated with radiating elements so that beam control and/or scanning may be realized. Because of the limited amount of available space in high frequency arrays, some authors have suggested the use of an active

patch antenna as the radiating element. By using active patch antennas, the problem of rf distribution to each radiating element is minimized and space is made available for phase shifters and power amplifiers.

In this paper, we report a first demonstration of a HTS/GaAs hybrid active patch antenna consisting of a hybrid oscillator on one substrate, and a feedline proximity coupled to a circular microstrip patch antenna on a second substrate. The patch antenna was printed on alumina ( $\epsilon_r = 9.9$ ) to reduce the effective permittivity seen by the radiator. The performance of this active antenna was measured at 77 K.

## II. DESIGN

Since our objective was to implement the entire oscillator on a single substrate to be cooled to 77 K, the  $S$ -parameters of the transistors were first obtained by measurements at cryogenic temperatures for use in the design of the oscillator. The active device used in the oscillator was a low noise MESFET with a gate length of  $0.25\text{ }\mu\text{m}$  (Toshiba GaAs MESFET, part no. JS8830-AS). The  $S$ -parameters of the FET for the frequency range of 2 GHz to 26 GHz were measured over a range from room temperature (300 K) to 40 K. The magnitude and angle of the  $S$ -parameters at 10 GHz as a function of temperature are shown in Fig. 1. The  $S$ -parameters as a function of frequency at 300 and 77 K will be presented elsewhere [8]. Of the  $S$ -parameters, the largest change in magnitude as a function of temperature occurred for the  $S_{21}$  values. This was due to an increase in the electron's mobility at the reduced temperatures. The variation in phase of  $S_{11}$  and  $S_{22}$  was the only other major change. The percent change of the magnitude and phase of the  $S$ -parameters at the design frequency of 10 GHz due to the change in the temperature from 300 K to 77 K is listed in Table I.

The oscillator was designed using simulations performed with a commercially available software package (Touchstone) under the assumption that the drain current would be held at  $I_d = 10\text{ mA}$ , and that the temperature would be held at 77 K. The design used a parallel coupled ring resonator in the matching network off the drain for the frequency stabilization. Using the small signal  $S$ -parameters that were measured at 77 K, the input reflection coefficient at the drain was made very large by

Manuscript received August 17, 1992; November 23, 1992. This work was supported by the National Aeronautics and Space Administration under award no. NCC-3-197. M. A. Richard was supported through the Ohio Aerospace Institute Doctoral Fellowship.

N. J. Rohrer and G. J. Valco are with the Department of Electrical Engineering, The Ohio State University, Columbus, OH 43210.

M. A. Richard is with the Department of Electrical Engineering, Case Western Reserve University, Cleveland, OH 44106.

K. B. Bhasin is with the National Aeronautics and Space Administration, Lewis Research Center, Cleveland, OH 44135.

IEEE Log Number 9206629.

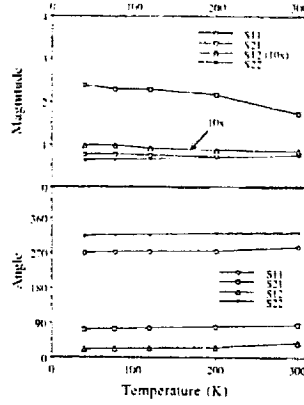


Fig. 1. Magnitude and angle of the  $S$ -parameters of the GaAsFET at 10 GHz as a function of temperature. The magnitude of  $S_{12}$  has been magnified by a factor of 10 for clarity.

TABLE I  
PERCENT CHANGE OF THE  $S$ -PARAMETERS FROM  
300 K TO 77 K AT 10 GHz

$S_{11}$		$S_{21}$		$S_{12}$		$S_{22}$	
Magnitude	Phase	Magnitude	Phase	Magnitude	Phase	Magnitude	Phase
3.4%	16.2%	25.6%	8.4%	4.8%	6.2%	26.7%	27.1%

varying the length of the transmission lines on the source and the gate. The selected lengths of the transmission lines from the source and gate were 1.57 mm and 2.79 mm, respectively. Both were open circuited lines. The ring resonator, with a fundamental resonant frequency of 10 GHz, which was used to select the frequency of operation was placed  $\lambda_g/4$  from the drain of the transistor, parallel coupled to the output transmission line using a 40- $\mu\text{m}$  wide coupling gap. The matching network, including the ring resonator, was designed such that the magnitude of the real part of the impedance of the matching network was less than the magnitude of the real part of the impedance looking into the drain of the FET. The magnitude of the imaginary part of the impedance was equal to zero at the resonant frequency. With this criterion met, the 10-GHz oscillation will start upon proper biasing of the FET. The output of the oscillator was taken off the drain. The physical layout of this reflection mode oscillator is shown in Fig. 2.

The antenna used for this investigation was a circular microstrip patch which was proximity coupled to a microstrip feedline. The feedline for the antenna was patterned on a second substrate for two reasons: this method allowed for the testing of both the oscillator and the antenna separately to determine their performance, and secondly, a HTS thin film with an area large enough to pattern the entire circuit was available.

The resonant frequency of the circular antenna patch was found from the formula [9]:

$$f = \frac{1.841c}{2\pi a_e \sqrt{\epsilon_{eq}}} \quad (1)$$

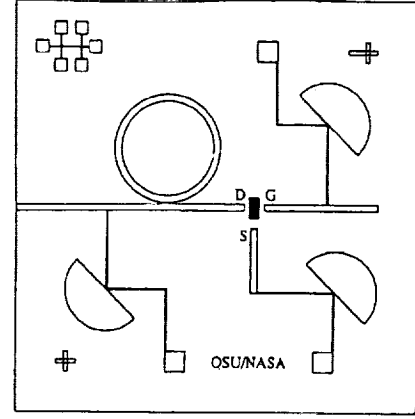


Fig. 2. Physical layout of the hybrid 10 GHz superconductor/GaAs oscillator designed using the reflection method.

where  $a_e$  is the effective radius of the patch

$$a_e = a \left[ 1 + \frac{2d}{\pi a \epsilon_{eq}} \left( \ln \frac{a}{2d} + (1.41 \epsilon_{eq} + 1.77) + \frac{d}{a} (0.268 \epsilon_{eq} + 1.65) \right) \right]^{1/2} \quad (2)$$

Here,  $d$  is sum of the thickness of the two substrates between the patch and the ground plane and  $a$  is the physical radius of the patch. Because the patch was printed on an alumina ( $\epsilon_1 = 9.9$ ) substrate with a thickness of 254  $\mu\text{m}$  while the feedline and ground plane were on lanthanum aluminate ( $\epsilon_2 = 23$ ) with a thickness of 508  $\mu\text{m}$ , the value for the net  $\epsilon_{eq}$  of this dual layer substrate to use in (1) and (2) was found using a static capacitor model

$$\epsilon_{eq} = \frac{3\epsilon_1\epsilon_2}{2\epsilon_1 + \epsilon_2} \quad (3)$$

to be 16.0, resulting in the diameter of the patch equaling 4.02 mm. Measurements showed that a slightly larger diameter of 4.71 mm resulted in a resonance closer to the desired frequency of 10 GHz. The resonant frequency of the patch was tuned to match the output frequency of the oscillator by adjusting the position of the patch over the feedline.

### III. EXPERIMENTAL DETAILS

An HTS film was patterned into the oscillator using standard positive photolithographic techniques and etched with an aqueous solution of deionized water :  $\text{H}_3\text{PO}_4 :: 100 : 1$ . This film was a commercially purchased film deposited using an off-axis sputtering technique and had a critical temperature of 88.6 K after patterning. Contacts to the superconductor for the rf output and wire bonding pads were made of silver with a gold overlayer patterned by lift-off photolithography. Wire bonding pads were located at the bias pads as well as at the ends of the transmission lines near the FET. The GaAs FET was epoxied onto the substrate and wire bonds were made to

the transmission lines with 0.7 mil gold wire by thermosonic bonding. A copper ground plane with a thickness of  $2.4\ \mu\text{m}$  was deposited on the backside of the substrate.

A second HTS thin film was used for the antenna feedline. A  $\text{YBa}_2\text{Cu}_3\text{O}_{7-x}$  thin film was deposited by pulsed laser deposition onto this substrate [10]. The film had a critical temperature of 86 K. This film was patterned in the same way as the oscillator into a 50 ohm transmission line that was  $160\ \mu\text{m}$  wide and 5 mm in length. A silver/gold contact was deposited at the end of the feedline for ribbon bonding, and a  $2\text{-}\mu\text{m}$  copper ground plane was evaporated on the backside of the substrate. An alumina substrate with the patterned antenna patch was placed on top of the feedline and held in place with small amounts of fingernail polish at the edges.

The performance of the oscillator was measured on a spectrum analyzer at 77 K by mounting the circuit in a sealed brass test fixture and submerging the fixture in liquid nitrogen. Details of the procedures used for measurement will be presented elsewhere [8]. The antenna with its HTS feedline was measured by placing the circuit on a copper test fixture and mounting the fixture on the second stage of a closed cycle gas refrigerator. A high density polyethylene radome served as a vacuum chamber. Details of the experimental apparatus and procedures have been presented elsewhere [5].

The efficiency of the antenna together with its HTS feedline was measured using the Wheeler Cap method [11]. To do this, the input impedance of the antenna at resonance was measured with and without a radiation shield from 30 K up to 85 K. The efficiency ( $\eta$ ) was then calculated as:

$$\eta = 1 - \frac{R_w}{R_{wo}} \quad (4)$$

where  $R_w$  and  $R_{wo}$  are the input resistances with and without the radiation shield, respectively. For this work, an aluminum cap with an inner dimension of 12-mm wide  $\times$  12-mm deep by 6.8 mm high was used as the radiation shield. Electrical contact to the test fixture was ensured with silver paint.

The oscillator and antenna circuits were then mounted with silver paint onto a brass test fixture. The rf connection between the two substrates was made by ribbon bonding to the contacts on the feedline of antenna and the output of the oscillator (Fig. 3). The test fixture was then mounted in the closed-cycle gas refrigerator and covered with the high density polyethylene radome. An X-band horn attached to a pivoting arm served as the receive antenna to measure the radiation pattern of the active patch antenna in the far field as a function of angle.

#### IV. RESULTS AND DISCUSSION

The output power and frequency of operation of the hybrid oscillator were measured to verify its performance before bonding the oscillator to the antenna circuit. The maximum power attainable from the oscillator at 77 K

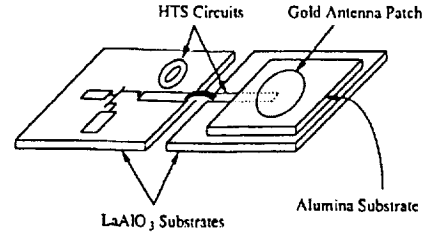


Fig. 3. Physical layout of the active antenna. The gold patch was on an alumina substrate placed over a superconducting feedline on a  $\text{LaAlO}_3$  substrate. The oscillator and patch antenna were ribbon bonded together.

was 11.5 dBm at a bias of  $V_{ds} = 4.0\ \text{V}$  and  $V_{gs} = 0.0\ \text{V}$ . The sensitivity of the frequency to temperature was  $-10\ \text{MHz/K}$  at 77 K. Detailed results of the measurements performed on this oscillator as a function of temperature and bias will be presented elsewhere [8]. For the active antenna measurements at 77 K, the FET was biased at  $V_{ds} = 0.5\ \text{V}$  and  $V_{gs} = -0.5\ \text{V}$  which gave a current of  $I_d = 12\ \text{mA}$ . For this bias condition, the frequency of the signal was 10.082 GHz with an output power of  $-2.0\ \text{dBm}$ . The efficiency of the oscillator was 10.5%. The power of the second harmonic at 20.16 GHz was 35 dB less than the fundamental signal at 77 K.

The efficiency of the antenna was measured before bonding the antenna to the oscillator circuit. The efficiency as a function of temperature is shown in Fig. 4. As expected, the efficiency rises dramatically as the HTS film becomes superconducting and then increases slowly as the temperature decreases, due to the increase in the conductivity of the HTS feedline. This trend was in agreement with the measured performance of HTS ring resonators. The efficiency reaches a maximum of 87.4% at 30 K.

The measured antenna patterns with the superconducting oscillator driving the antenna are shown in Fig. 5, along with the patterns predicted for the co-polarization by the cavity model [12]. The  $H$ -plane shows good agreement with the model, while the  $E$ -plane deviates substantially due to surface waves and the feedline, neither of which are accounted for in the model used. This is in agreement with results published by Schaubert *et al.* [13] which demonstrated that antennas on high permittivity substrates are characterized by perturbations in the  $E$ -plane pattern. The 12 dB dip in the  $E$ -plane and the cross polarization patterns at an angle of 15 degrees was almost certainly due to radiation interference from the resonator and microstrip lines on the oscillator.

#### V. CONCLUSION

The performance of a 10 GHz active antenna employing a Y-Ba-Cu-O superconducting feedline and resonator stabilized oscillator has been demonstrated for the first time. The patch antenna and the hybrid oscillator were fabricated on separate  $\text{LaAlO}_3$  substrates. The measurements on the antenna showed that it was 71% efficient at 77 K and 87.4% efficient at 30 K. The oscillator had a maximum power of 11.5 dBm and was 10.5% efficient at

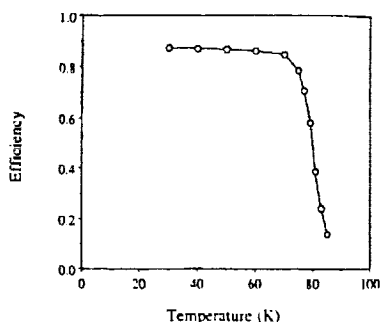


Fig. 4. Efficiency of the patch antenna as a function of temperature measured from 30 K to 85 K. The efficiency at 77 K was 71%.

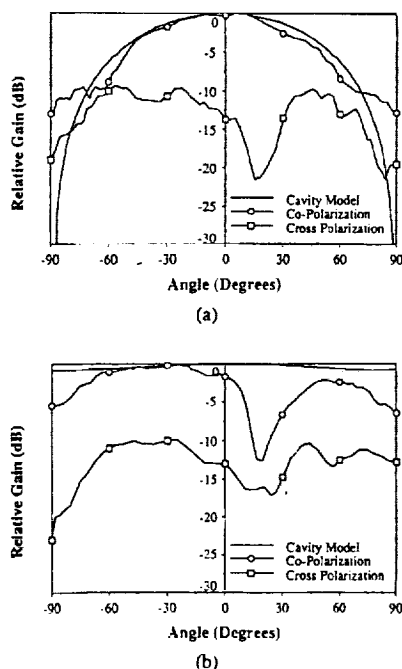


Fig. 5. Radiation patterns for the patch antenna at 77 K. a) *H*-plane radiation patterns comparing the cavity model (solid line) with the co-polarization data (open circles) and also displaying the cross polarization data (open squares). b) *E*-plane radiation patterns comparing the cavity model with the co-polarization data and also displaying the cross polarization data.

77 K. The sensitivity of the frequency as a function of temperature was  $-10$  MHz/K. The radiation patterns for the oscillator were measured as a function of the angle and compared to a cavity model for a driving power from the oscillator of  $-2.0$  dBm. The *H*-plane showed good agreement with the model, while interference due to the oscillator was present in each trace except the co-polarization of *H*-plane.

#### ACKNOWLEDGMENTS

The authors would like to thank Chris Chorey for his assistance in the testing of the transistor at cryogenic temperatures.

#### REFERENCES

- [1] C. M. Chorey, K. Kong, K. B. Bhasin, J. D. Warner, and T. Itoh, "YBCO Superconducting ring resonator at millimeter-wave frequencies," *IEEE Trans. Microwave Theory Tech.*, vol. 39, no. 9, pp. 1480-1487, Sept. 1991.
- [2] J. H. Takemoto, F. K. Oshita, H. R. Fetterman, P. Korbin, and E. Sovoro, "Microstrip ring resonator technique for measuring microwave attenuation in high- $T_c$  superconducting thin films," *IEEE Trans. Microwave Theory Tech.*, vol. 37, pp. 1650-1652, 1989.
- [3] W. G. Lyons, R. R. Bonetti, A. E. Williams, P. M. Mankiewicz, M. L. O'Malley, J. M. Hamm, A. C. Anderson, R. S. Withers, A. Meulenberg, and R. E. Howard, "High- $T_c$  superconductive microwave filters," *IEEE Trans. Magn.*, vol. 27, no. 2, pp. 2537-2539, Mar. 1991.
- [4] E. B. Ekholm and S. W. McKnight, "Attenuation and dispersion for high- $T_c$  superconducting microstrip lines," *IEEE Trans. Microwave Theory Tech.*, vol. 38, no. 4, pp. 387-395, Apr. 1990.
- [5] M. A. Richard, K. B. Bhasin, C. Gilbert, S. Metzler, G. Keopf, and P. C. Claspy, "Performance of a four-element Ka-band high-temperature superconducting microstrip antenna," *IEEE Microwave Guided Wave Lett.*, vol. 2, no. 4, pp. 143-145, Apr. 1992.
- [6] R. J. Dinger, "Some potential antenna applications of high temperature superconductors," *J. Superconduct.*, vol. 3, no. 3, pp. 287-196, 1990.
- [7] R. C. Hansen, "Superconducting antennas," *IEEE Trans. Aerospace Electronic Syst.*, vol. 26, no. 2, pp. 345-354, Mar. 1990.
- [8] N. J. Rohrer, G. J. Valco, and K. B. Bhasin, "Hybrid high temperature superconductor/GaAs 10 GHz microwave oscillator: Temperature and bias effects," *IEEE Trans. Microwave Theory Tech.*, (Accepted for publication).
- [9] W. C. Chew and J. A. Kong, "Effects of fringing fields on the capacitance of circular microstrip disks," *IEEE Trans. Microwave Theory Tech.*, vol. 28, no. 2, pp. 98-104, Feb. 1990.
- [10] J. D. Warner, K. B. Bhasin, N. J. Varlaj, D. Y. Bowman, and C. M. Chorey, "Growth and patterning of laser ablated superconducting YBCO films on LaAlO<sub>3</sub> substrates," NASA Report No. TM-102336.
- [11] H. A. Wheeler, "The radiansphere around a small antenna," *Proc. IRE*, vol. 47, pp. 1325-1331, Aug. 1959.
- [12] I. J. Bhal and P. Bhartia, *Microstrip Antennas*, Massachusetts: Artech House, 1980.
- [13] D. H. Schaubert and K. S. Yngvesson, "Experimental study of a microstrip array on high permittivity substrate," *IEEE Trans. Antennas Propag.*, vol. 34, no. 1, pp. 92-97, Jan. 1986.



Norman J. Rohrer received the B.S. degree in physics and mathematics from Manchester College, North Manchester, Indiana in 1987, and the M.S. and Ph.D. degrees in electrical engineering from the Ohio State University, Columbus, Ohio, in 1990 and 1992, respectively.

As a graduate student, he was recipient of a NASA Graduate Student Research Fellowship under which he was able to complete his dissertation research on superconducting microwave oscillators. Since August of 1992, he has been

employed by IBM, Burlington, Vermont, in the Technology Products Division.



M. A. Richard (S'92) received the B.A. in physics from Bluffton College in 1988 and the M.S. and Ph.D. degrees in electrical engineering from Case Western Reserve University in 1990 and January, 1993, respectively.

He was a recipient of an Ohio Aerospace Institute/NASA Space Grant Doctoral Fellowship. Dr. Richard has co-authored 15 technical papers, one of which won first place at the IEEE Antennas and Propagation Society's 1992 Student Paper Contest. He is currently a Research

Associate at Case Western Reserve University where he is continuing his investigation of superconducting antennas.

**George J. Valco (M'86)** received the B.S. and M.S. degrees in electrical engineering from Case Western Reserve University in 1979 and 1981, respectively. He received the Ph.D. in electrical engineering from the University of Cincinnati in 1986.

In 1986 he joined the faculty of the Ohio State University where he is currently an assistant professor of electrical engineering. His current research interests are electronic applications of high temperature superconductors, electronic properties of diamond films, photovoltaics, and compound semiconductor devices and technology.

**Kul B. Bhasin (S'74-M'83-SM'89)** received the M.S. and Ph.D. degrees from Purdue University and the University of Missouri-Rolla, respectively.

Since 1983 he has been a senior research scientist in the Solid State Technology Branch of the Space Electronics Division of the NASA Lewis Research Center in Cleveland, Ohio. Prior to joining NASA he was with Gould, Inc. from 1977 to 1983 as senior scientist and manager of technology. He is currently engaged in development of GaAs microwave devices and circuits, microwave photonics and superconducting electronics for space applications. He has authored many publications and co-edited the book, *Microwave Integrated Circuits*. He is the recipient of the IR-100 Award, the NASA Group Achievement Awards, the Gould Scientific Achievement Award and is on the editorial board of *Microwave and Optical Technology Letters*. He is a member of APS, Sigma Xi, and a member of the Fellow International Society for Optical Engineers.



# PERFORMANCE OF $\text{TiCaBaCuO}$ 30 GHz 64 ELEMENT ANTENNA ARRAY

L. L. Lewis and G. Koepf  
Ball Communications Systems Division,  
Broomfield, CO 80038-1235  
K. B. Bhasin  
NASA Lewis Research Center,  
Cleveland, OH 44135  
M. A. Richard  
Case Western Reserve University,  
Cleveland, OH 44106

**Abstract**—A 64 element, 30 GHz, microstrip antenna array with corporate feed network was designed and built on a .254 mm (10 mil) thick lanthanum aluminate substrate. One antenna pattern was fabricated from gold film, and a second pattern used  $\text{TiCaBaCuO}$  high temperature superconductor. Both antennas used gold ground planes deposited on the reverse side of the substrate. Gain and radiation patterns were measured for both antennas at room temperature and at cryogenic temperatures. Observations agree well with simple models for loss and microwave beam width, with a gain on boresight of 20.3 dB and beam width of 15 degrees for the superconducting antenna.

## I. INTRODUCTION

When microstrip antenna design [1] is extended to microwave frequencies above 30 GHz, certain difficulties become apparent. Losses due to surface waves [2] and radiation [3] become more significant than at lower frequencies. Both of these losses may be reduced by decreasing the thickness of the substrate, drawing the ground plane closer to the microstrip traces. However, the trace widths must also be reduced in order to maintain a given transmission line impedance. The narrower lines have high resistive losses when conventional metals are used to form the traces. For copper traces on a .152 mm (6 mil) thick sapphire substrate, for example, a 30 GHz phased array with 40 dB directivity will have more than 25 dB of loss [4]. In order to reduce these resistive losses, high temperature superconducting (HTS) materials may be used to form the feed networks for high gain phased array antennas [5]. When a high quality HTS film on .254 mm (10 mil) lanthanum aluminate (LAO) is used instead of copper for a 30 GHz antenna of 40 dB directivity, the loss is only 3 dB [4]. This paper describes the design, construction, and performance of the first 30 GHz, 64 element phased array antenna that uses an HTS feed network. The successful implementation of HTS circuits with this relatively low gain antenna supports the position that high gain millimeter wave antennas would benefit from use of the new superconductors.

Manuscript received August 24, 1992. Research supported in part by NASA Headquarters, Satellite Communications Applications Research (SCAR) Program.

© 1993 IEEE. Reprinted, with permission, from IEEE Transactions on Applied Superconductivity, vol. 3, no. 1, Mar. 1993, pp. 2844-2847.

## II. ANTENNA DESIGN

### A. General Design

For ease in fabrication, and in order to compare HTS performance with copper performance, we selected an array design with 64 rectangular patches arranged in an  $8 \times 8$  square pattern (Fig. 1). Element spacing was 4500  $\mu\text{m}$ , which is slightly less than one-half of the free space wavelength. This reduced spacing allowed us to place the entire array on a 50.8 mm (2 inch) diameter wafer of LAO, without appreciably changing the radiation pattern of the antenna. Wafer thickness was chosen to be .254 mm (10 mils), with a gold ground plane on the reverse side. The corporate feed network uses 50 ohm lines, which are split to the patch elements by means of six levels of quarter wave microstrip transformers. The relative dielectric constant of LAO is approximately 24 [6], which results in a microstrip line width of 92  $\mu\text{m}$  for this geometry.

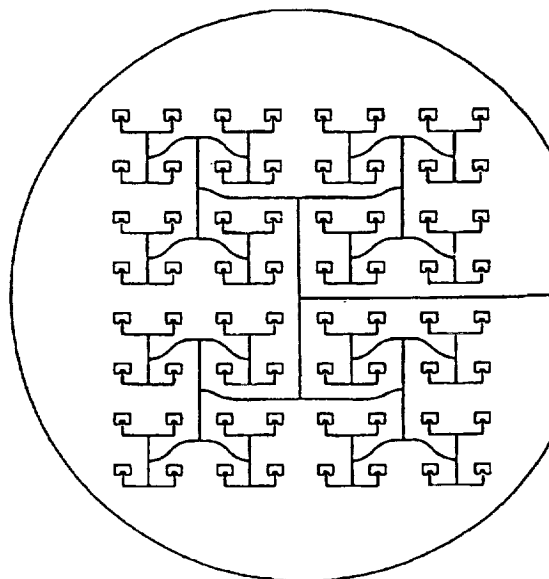


Fig. 1 Layout of patch elements and feed network for the 30 GHz phased array antenna. Wafer diameter is 50.8 mm (2 inches).

## B. Antenna Patch Elements

Because of the uncertainty in material properties and the application of microwave design rules for substrates with such high dielectric constant, we designed, fabricated, and tested single patches at 15 GHz first, in order to determine the validity of our models for devices on LAO at MMW frequencies. We then extended the design to 30 GHz patches, which were then used in arrays. The patches are rectangular, with width  $W$  and length  $L$  (Fig. 2). A microstrip line feeds directly to a notched input of depth  $d$ . The calculation of the patch resonance frequency is not difficult, but an accurate calculation of patch impedance is nontrivial. We use a Mixed Potential Integral Equation (MPIE) approach [7]. This is one of several 'full wave' models, which should give good values for patch impedance, surface wave components, and radiation patterns. The patch impedance is needed in order to couple the microwave power efficiently into the patch. The antenna efficiency is determined in part by the resistive losses of the patch, and also by the energy lost to surface waves.

The edge impedance of a rectangular patch on LAO is very high, requiring the use of the notch, which allows coupling near the center of the patch, where the impedance goes to zero. We select a point where the impedance is 100 ohms, and use a quarter wave transformer to match the 50 ohm input line to this point. Typical values are  $W=3000\text{ }\mu\text{m}$ ,  $L=2000\text{ }\mu\text{m}$ , and  $d=782\text{ }\mu\text{m}$  for a resonance frequency of 14.84 GHz, and theoretical input impedance of 78 ohms. The measured impedance in this case was 72 ohms. For the 64 element array, we used patches with  $W=1350\text{ }\mu\text{m}$ ,  $L=900\text{ }\mu\text{m}$ , and  $d=337\text{ }\mu\text{m}$ . These elements have a predicted resonance frequency of 31.25 GHz, and input impedance of 100 ohms.

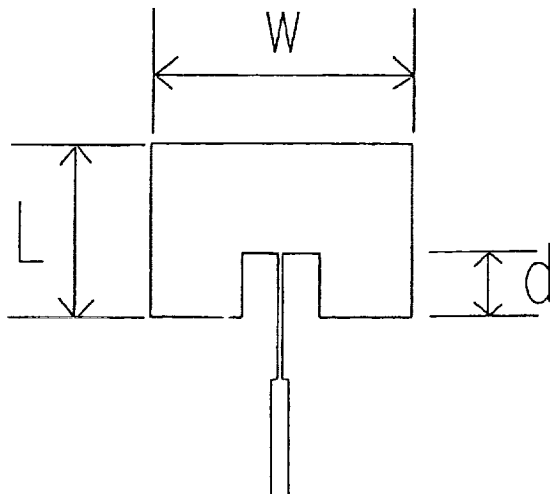


Fig. 2 Antenna patch element, showing quarter wave input transformer.

## C. Surface Waves

The high dielectric constant of LAO means that even a .254 mm (10 mil) substrate is electrically thick. While the cutoff frequency for propagation of the  $TE_0$  surface wave mode is about 60 GHz, the  $TM_0$  mode is supported at all frequencies. This can be a source of energy loss. We have calculated the radiation efficiency of a single patch, using an electric surface current model [8] to estimate the surface wave losses. At 15 GHz, the single patch efficiency is about 84 percent. At 30 GHz, the efficiency drops to about 60 percent.

In theory, the efficiency of an array can be improved considerably over this value by carefully placing the radiating elements at the correct distance apart, so that the surface wave components destructively interfere. The spacing can also be chosen so that the spatial part of the radiation constructively interferes. Both are possible at the same time because the wavelength of the surface waves is nearly one fifth of the free space wavelength. In practice, however, the presence of the feed network makes it difficult to predict the exact propagation constants in the structure, so that surface waves can be suppressed.

## III. FABRICATION

The preliminary single patches at 15 GHz and 30 GHz were fabricated at Ball using 4  $\mu\text{m}$  thick gold on .254 mm (10 mil) thick LAO, with a titanium adhesion layer. Both plate up and etch down processes were used. Gold ground planes were deposited on the reverse side of the LAO. The diced patches were soldered with indium to gold plated metal carriers made of Alloy 48, which matches the coefficient of thermal expansion of the LAO. The carriers were then mounted in a test fixture, using gold ribbon bonds to microstrip launchers, which in turn were bonded to 'V-type' microwave connectors.

The 64 element array was patterned by Superconductor Technologies, Inc. on a 50.8 mm (2 inch) diameter, .254 mm (10 mil) thick LAO. One array was formed with 3  $\mu\text{m}$  thick gold film, using a titanium-tungsten adhesion layer, and a second array was formed with  $Tl_2CaBa_2Cu_2O_8$  high temperature superconductor. Both arrays used a gold ground plane deposited on the reverse side of the LAO. The 50 ohm microstrip feed line, as shown in Fig. 1, passes to the edge of the wafer, where a gold ribbon bond is made to a microstrip launcher. In the case of the HTS array, a gold contact strip is deposited over the superconductor near the end of the wafer, for bonding purposes. As with the single patches, the wafer is soldered to a gold plated fixture using an indium alloy. On both the gold and the HTS arrays, line widths were held to a tolerance of about 3  $\mu\text{m}$ . Substrate thickness variations were less than .025 mm (1 mil).



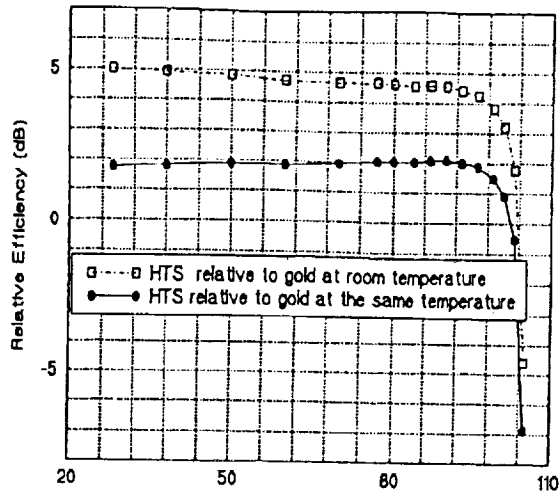


Fig. 3 Efficiency of HTS antenna relative to gold antenna.

#### IV. PERFORMANCE

The resonance frequency of both the gold and the HTS arrays was measured at Ball, at both room temperature and liquid nitrogen temperatures. The gold array was resonant at 30.7 GHz (room temperature) and 31.1 GHz (77 K). The HTS array was resonant at 30.55 GHz (77 K). A calibrated gain measurement of the gold array was made at Ball, at room temperature. The measured gain, on resonance and on boresight was 15.6 dBil (H-plane). The 3 dB beam width was 13 degrees. The relative gain of the gold and HTS antennas at cryogenic temperatures was then measured at NASA Lewis Research Center. We express the normalized gain,  $G$ , of an antenna in terms of the usual S-parameters:

$$G = \frac{|S_{21}|^2}{1 - |S_{11}|^2} \quad (1)$$

Then the efficiency of the HTS antenna relative to the gold antenna is just

$$\epsilon_{HTS-Au} = G_{HTS} / G_{Au} \quad (2)$$

Fig. 3 gives the efficiency of the HTS antenna relative to the gold antenna at 300 K and also relative to the gold antenna at the same temperature as the HTS antenna. At 77 K, the HTS antenna is 4.7 dB higher gain than the gold antenna at room temperature. We therefore conclude, using the calibrated gain measurements of the gold antenna, that the gain of the HTS antenna at 77 K is 20.3 dB. This is to be compared with the maximum possible gain (no losses) of 22.2 dB. The

inferred loss of 1.9 dB can easily be attributed to losses in the microwave connectors, gold ground plane, and surface waves. Indeed, the predicted maximum loss due to surface waves alone is 2.2 dB. Using a simple model of resistive losses in the feed network, we expect the gold antenna losses at 300 K to be 3.8 dB, and 2.2 dB at 77 K. Similarly, we expect the HTS losses to be .4 dB at 77 K. The measured gains are in reasonable agreement with these estimates.

Fig. 4 and Fig. 5 give the E-plane and H-plane radiation pattern measurements for the HTS antenna at 77 K. These two measurements are in excellent agreement with the predicted patterns, showing the first side lobes at -13 dBc, with good symmetry. The slight skewing of the central lobe may be attributed to asymmetry in the measurement fixture.

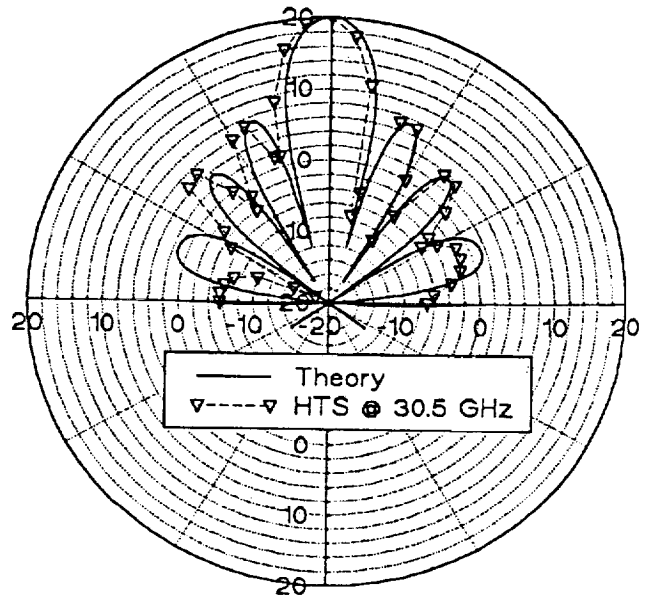


Fig. 4 E-plane radiation pattern, normalized to 20 dB.

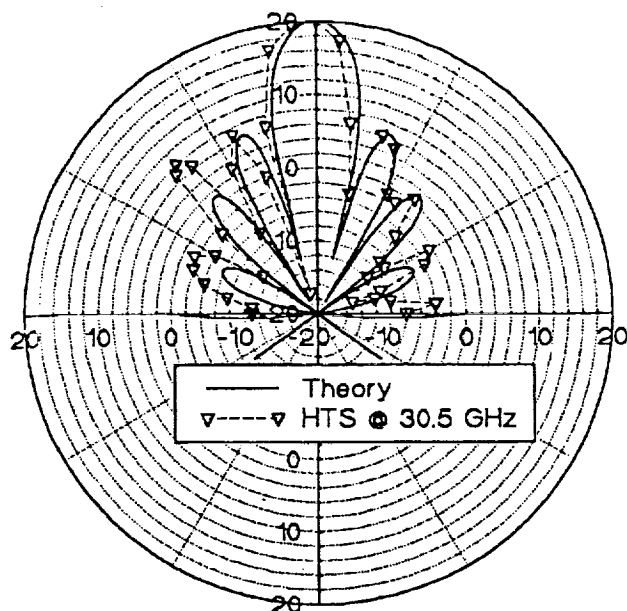


Fig. 5 H-plane radiation pattern, normalized to 20 dB.

## V. SUMMARY

The measured performance of a 30 GHz, 64 element phased array antenna with a superconducting feed network agrees well with theory. The antenna loss is only 1.9 dB, and the radiation patterns behave as predicted. These results support the contention that significant gain improvements are possible in a high gain millimeter wave antenna that uses an HTS feed network.

## REFERENCES

- [1] P. Bhartia, K. V. S. Rao, and R. S. Tomar, *Millimeter-Wave Microstrip and Printed Circuit Antennas*, Boston: Artech House, 1991, 322 pp.
- [2] Pisti B. Katehi and Nicolaos G. Alexopoulos, "On the Effect of Substrate Thickness and Permittivity on Printed Circuit Dipole Properties," *IEEE Trans. on Antennas and Propagation*, Vol. AP-31, No. 1, pp. 34-39, January, 1983.
- [3] L. Lewin, "Radiation from Discontinuities in Stripline," *IEEE Monograph No. 358E*, February 1960.
- [4] Fred Schmidt, "Superconducting Antennas Applications and Architecture Study," Final Report, NASA contract No. NASW-4514, August, 1991, pp. 49-53.

- [5] M. A. Richard, K. B. Bhasin, C. Gilbert, S. Metzler, and P. C. Claspy, "Measurement techniques for cryogenic Ka-Band microstrip antennas," *Antenna Measurement Tech. Association Proc.*, pp. 1.13-1.17, 1991.
- [6] Tsuneo Konaka, Makoto Sato, Hidefumi Asano, and Shugo Kubo, "Relative Permittivity and Dielectric Loss Tangent of Substrate Materials for High- $T_c$  Superconducting Film," *Journal of Superconductivity*, Vol. 4, No. 4, pp. 283-288, 1991.
- [7] J. R. Mosig, "Arbitrarily Shaped Microstrip Structures and their Analysis with a Mixed Potential Integral Equation," *IEEE Trans. Microwave Theory and Techniques*, Vol. 36, No. 2, pp. 314-323, February 1988.
- [8] P. Perlmutter, S. Shtrikman, and D. Treves, "Electric Surface Current Model for the Analysis of Microstrip Antennas with Application to Rectangular Elements," *IEEE Transactions on Antennas and Propagation*, Vol. AP-33, No. 3, pp. 301-311, March 1985.